

ASC Report No. 37/2014

Whispering gallery modes in oblate spheroidal cavities: calculations with a variable stepsize

P. Amodio, T. Levitina, G. Settanni, E. Weinmüller

Institute for Analysis and Scientific Computing —
Vienna University of Technology — TU Wien
www.asc.tuwien.ac.at ISBN 978-3-902627-05-6

Most recent ASC Reports

- 36/2014 *J. Burkotova, I. Rachunkova, S. Stanek and E. Weinmüller*
Analytical and numerical treatment of singular linear BVPs with unsmooth inhomogeneity
- 35/2014 *E. Weinmüller*
Collocation - a powerful tool for solving singular ODEs and DAEs
- 34/2014 *M. Feischl, T. Führer, G. Gantner, A. Haberl, D. Praetorius*
Adaptive boundary element methods for optimal convergence of point errors
- 33/2014 *M. Halla, L. Nannen*
Hardy space infinite elements for time-harmonic two-dimensional elastic waveguide problems
- 32/2014 *A. Feichtinger and E. Weinmüller*
Numerical treatment of models from applications using BVPSUITE
- 31/2014 *C. Abert, M. Ruggeri, F. Bruckner, C. Vogler, G. Hrkac, D. Praetorius, and D. Suess*
Self-consistent micromagnetic simulations including spin-diffusion effects
- 30/2014 *J. Schöberl*
C++11 Implementation of Finite Elements in NGSolve
- 29/2014 *A. Arnold and J. Erb*
Sharp entropy decay for hypocoercive and non-symmetric Fokker-Planck equations with linear drift
- 28/2014 *G. Kitzler and J. Schöberl*
A high order space momentum discontinuous Galerkin method for the Boltzmann equation
- 27/2014 *W. Auzinger, T. Kassebacher, O. Koch, and M. Thalhammer*
Adaptive splitting methods for nonlinear Schrödinger equations in the semiclassical regime

Institute for Analysis and Scientific Computing
Vienna University of Technology
Wiedner Hauptstraße 8–10
1040 Wien, Austria

E-Mail: admin@asc.tuwien.ac.at
WWW: <http://www.asc.tuwien.ac.at>
FAX: +43-1-58801-10196

ISBN 978-3-902627-05-6

© Alle Rechte vorbehalten. Nachdruck nur mit Genehmigung des Autors.



Whispering gallery modes in oblate spheroidal cavities: calculations with a variable stepsize

P. Amodio*, T. Levitina[†], G. Settanni,** and E. B. Weinmüller[‡]

*Dipartimento di Matematica, Università di Bari, I-70125 Bari, Italy

[†]Institut Computational Mathematics, TU Braunschweig, D-38106 Braunschweig, Germany

**Dipartimento di Matematica e Fisica 'E. De Giorgi', Università del Salento, I-73047 Lecce, Italy

[‡]Vienna University of Technology, Institute for Analysis and Scientific Computing, A-1040 Wien, Austria

Abstract. We propose an efficient and reliable technique to calculate highly localized Whispering Gallery Modes (WGMs) inside an oblate spheroidal cavity. The idea is to first separate variables in spheroidal coordinates and then to deal with two ODEs, related to the angular and radial coordinates solved using high order finite difference schemes. It turns out that, due to solution structure, the efficiency of the calculation is greatly enhanced by using variable stepsizes to better reflect the behaviour of the evaluated functions. We illustrate the approach by numerical experiments.

Keywords: Multiparameter spectral problems; Prüfer angle; finite difference schemes; variable stepsize

PACS: 02.30.Hq, 02.30.Jr, 02.60.Cb, 02.60.Lj, 02.70.Bf

INTRODUCTION

Recently [4], we reported on the progress in the calculations of the Whispering Gallery Modes inside a prolate spheroidal cavity. The calculation of such modes is difficult, since the model equation exhibits full variety of oscillations, while the WGMs are localized inside a very narrow strip in the near-equatorial domain of a cavity and show extremely large gradients inside this exited domain. When computing WGMs directly, one has not only to calculate rapidly changing solutions, but also to perform a tiresome selective work, choosing the WGM eigen-frequencies among thousands or millions of others. Fortunately, the scalar Helmholtz equation is separable in spheroidal coordinates and therefore, the eigen-oscillations can be represented as a product of components each depending on its own single variable. The search of highly localized oscillations is easy to formulate in terms of separated equations: only those modes are of interest that are formed by exactly one fast oscillating component, while the remaining components are practically non-oscillatory.

OBLATE SPHEROIDAL COORDINATES AND OBLATE SPHEROIDAL WAVE FUNCTIONS

Following [6], we introduce the oblate spheroidal coordinates ξ, η, ϕ via their relations to the Cartesian coordinates:

$$x = \frac{d}{2} \sqrt{(\xi^2 + 1)(1 - \eta^2)} \cos \phi, \quad y = \frac{d}{2} \sqrt{(\xi^2 + 1)(1 - \eta^2)} \sin \phi, \quad z = \frac{d}{2} \xi \eta.$$

Here $\xi \in [0, \infty)$, $\eta \in [-1, 1]$, $\phi \in [0, 2\pi)$. The corresponding coordinate surfaces are confocal one-sheeted hyperboloids of revolution and oblate spheroids, with d being the distance between the foci. The cavity of the resonator is bounded by the oblate spheroidal surface $\xi = \xi_s$.

The separation of variables leads to two oblate spheroidal wave equations, one depending on the radial (ξ) and the other on the angular (η) coordinate, respectively,

$$\frac{d}{d\eta} (1 - \eta^2) \frac{d}{d\eta} S + \left[\lambda - c^2 (1 - \eta^2) - \frac{m^2}{1 - \eta^2} \right] S = 0, \quad -1 < \eta < 1, \quad (1)$$

$$\frac{d}{d\xi} (\xi^2 + 1) \frac{d}{d\xi} R + \left[c^2 (\xi^2 + 1) - \lambda + \frac{m^2}{\xi^2 + 1} \right] R = 0, \quad 0 < \xi < \xi_s. \quad (2)$$

Though separated, these equations remain coupled through the separation constant λ and the eigen-frequency c , $c = kd/2$, with k being the wave number. The angular equation has two singular points, $\eta = \pm 1$. If a solution to the angular equation bounded at the endpoints of the interval exists, then it is either odd or even. This reduces the consideration of (1) posed on the half-interval $(0, 1)$ subject to one of the following boundary conditions sets:

$$S'(0) = 0, |S(\eta)| < \infty, \eta \rightarrow 1 \quad \text{or} \quad S(0) = 0, |S(\eta)| < \infty, \eta \rightarrow 1. \quad (3)$$

Note that the parity of the angular function reflects the parity of the entire solution of the Helmholtz equation [4]. If this solution exhibits oscillations concentrated around the equatorial line of the spheroid, assuming their maximum on the equator, then its angular part is an even function with $S'(0) = 0$. Also, the radial function must correspond to the parity of a solution to the Helmholtz equation.

The boundary conditions the solution of the Helmholtz equation satisfies on the surface of the spheroidal cavity provide the boundary conditions, either Dirichlet or Neumann, for the radial function R at $\xi = \xi_s$. This means

$$R'(0) = 0, R(\xi_s) = 0 \quad \text{or} \quad R'(0) = 0, R'(\xi_s) = 0. \quad (4)$$

Equations (1), (2) form a singular self-adjoint *two-parameter* Sturm–Liouville problem, combined with the four possible choices of the boundary conditions. From the theory on multi-parameter spectral problems [8] it is possible to prove that, for a fixed pair of indexes $l, n \in \mathbb{N}$, the functions $S_{ln}(\eta)$ and $R_{ln}(\xi)$ exist and satisfy (1), (2), where l and n represent the number of oscillations within their definition intervals, respectively. We note that in order to guarantee uniqueness, both angular and radial function are normalized by

$$\int_{-1}^1 S^2(\eta) d\eta = 1, \quad \int_1^{\xi_s} R^2(\xi) d\xi = 1. \quad (5)$$

BOUNDARY CONDITION IN THE SINGULAR POINT

Since (1) is symmetric with respect to 0 and singular in 1, we solve it on the interval $[0, 1 - \delta_\eta]$ for a fixed small $\delta_\eta > 0$. Here, the singularity at the point $\eta = 1$ is regular [5]. All bounded solutions of (1) at the singular point $\eta = 1$ satisfy the same modified logarithmic derivative $\beta_a(\eta)$ defined as $(1 - \eta^2) \frac{d}{d\eta} S(\eta) = \beta_a(\eta) S(\eta)$. We point out that the logarithmic derivative β_a of any solution to (1) satisfies the Riccati equation,

$$\beta'(\eta) + \frac{\beta^2(\eta)}{1 - \eta^2} + Q_a(\eta) = 0, \quad (6)$$

where $Q_a(\eta) = \lambda - c^2(1 - \eta^2) - \frac{m^2}{1 - \eta^2}$. In the vicinity of $\eta = 1$, β is expanded into the power series

$$\beta(\eta) = \sum_{k=0}^{\infty} \beta_k (1 - \eta)^k, \quad (7)$$

where $\beta_0 = \beta_a(1) = -m$ and $\beta_1 = -\beta'_a(1) = \frac{\lambda}{1+m}$ are known [7]. Consequently, using (7), boundary conditions for the equation (1) posed in the singular point $\eta = 1$, can be transferred to a closely located regular point $1 - \delta_\eta$.

NUMERICAL SOLUTION USING VARIABLE STEPSIZE FINITE DIFFERENCES

We follow the approach already used in [3, 4] to approximate the prolate spheroidal wave function, using the step adaptation strategy proposed in [1]. For the angular S and radial R equations, we consider grids with n_S and n_R (initially equidistantly spaced) points, respectively. Equations (1), (2) are discretized by means of finite difference schemes of high order given by

$$y^{(v)}(x_i) \simeq y_i^{(v)} = \frac{1}{h_{x,i}^v} \sum_{j=-s}^r \alpha_{s+j,s,r}^{(v)} y_{i+j}, \quad h_{x,i} = x_i - x_{i-1}, \quad (8)$$

where $\nu = 1, 2$ and $(x, y) = \{(\eta, S), (\xi, R)\}$. Here, $\alpha_{i,s,r}^{(\nu)}$ are the coefficients chosen to provide a possibly high consistency order and y_i are approximations for $S(\eta_i)$ or $R(\xi_i)$. The values of s and r are related to the order of the formula and its stability properties. Here, when possible, we choose $r = s$. Moreover, in the next section the considered method is of order 8.

The discretization of (1), (2) (the first equation is solved in $[0, 1 - \delta_\eta]$) together with boundary conditions (3), (4) and (7) (right condition posed in point $1 - \delta_\eta$) and the numerical approximation of the normalization conditions (5) give rise to the following discrete problem

$$((I - D_\eta^2)A_\eta - 2D_\eta B_\eta + \lambda I + c^2(I - D_\eta^2) - m^2(I - D_\eta^2)^{-1})S = 0, \quad (9)$$

$$((D_\xi^2 + I)A_\xi + 2D_\xi B_\xi + c^2(D_\xi^2 + I) - \lambda I + m^2(D_\xi^2 + I)^{-1})R = 0, \quad (10)$$

$$h_1 S^T D_1 S = 0, \quad (11)$$

$$h_2 R^T D_2 R = 0. \quad (12)$$

Here, (9) - (12) form the nonlinear $(n_S + n_R + 2) \times (n_S + n_R + 2)$ system for the unknowns $S = [S(\eta_1), S(\eta_2), \dots, S(\eta_{n_S})]$, $R = [R(\xi_1), R(\xi_2), \dots, R(\xi_{n_R})]$, λ , and c^2 . Matrices D_x are diagonal and contain the discretization of η and ξ , while the diagonal matrices D_1 and D_2 are related to the quadrature formulae approximating (5). Matrices A_x and B_x contain the coefficients of the methods. As in [3, 4] an initial approximation for λ and c^2 , with an error of 10^{-6} , is provided from the Prüfer angle technique. Therefore, we solve the decoupled problems (9) and (10) separately. Since now these problems are linear, we can start with only 20 equidistantly spaced grid points and obtain a first rough approximation for S and R , where for efficiency reasons the stepsizes are adapted to reflect the oscillations of the eigenvectors occurring only in a very small part of the interval. The step adaptation strategy is based on the equidistribution of the estimated absolute global error of the eigenvectors computed by using two methods of consecutive even order. Next, a Newton iterative method is applied to solve the complete nonlinear system (9) - (12) in order to solve for S , R , λ and c^2 simultaneously up to the desired accuracy. In this last phase the same mesh adaptation strategy is applied.

ADAPTING THE STEPSIZE

The mesh adaptation strategy is based on an estimate of the absolute global error in the angular and radial functions obtained using two finite difference schemes of different order. First, we assume that a good approximation for the parameter pair (λ, c^2) is available from the Prüfer angle technique. Then taking an initially constant stepsize for both integration domains, we solve the decoupled systems (9) and (10) and normalize the solution using (11) and (12) afterwards. The starting numerical approximation for S and R are computed using $n_S = n_R = 20$ equidistant points. Then the nonlinear problem (9) - (10) is solved two times using two methods of different order to provide the estimate for the discretization error in the angular and radial functions. The well-known idea of the error equidistribution results in a piecewise constant grid of n_S and n_R points clustered in N_S and N_R blocks with constant stepsizes h_t and h_τ , respectively, in the t -th and τ -th blocks, where $t = 1, \dots, N_S$, $\tau = 1, \dots, N_R$. This numerical procedure is carried out until the desired accuracy TOL is satisfied. We point out that the nonlinear system (9) - (12) is solved iteratively using the Newton method, which works very well, because the starting approximation for (λ, c^2) has an adequate quality.

NUMERICAL SIMULATION

We have performed several numerical tests to illustrate the performance in case of constant and variable meshes. We have focused our attention on small values of l and n , where the solution is essentially zero in almost all the domain, see FIGURE 1, where two models with $l = n = 0$ and $l = n = 2$ are considered. The azimuthal mode number, m , related to the fast oscillating component $e^{im\varphi}$ was chosen between $m = 100$ and $m = 500$. In TABLE 1, we compare the methods using constant and variable grids. We have first solved five model problems on adapted grids using the strategy described in the pervious sections. The starting meshes were uniform with $n_S = n_R = 20$ points and we used a method of order 8 until the $TOL = 10^{-8}$ has been satisfied. These results are highlighted bold face. The absolute errors for the angular and radial functions and the relative errors for the parameters (λ, c^2) are also specified. Then, we have solved the problems using constant meshes with the same number of points to see how the accuracy deteriorates. These results are displayed below the bold face line. The estimated number of the required equidistant points necessary to obtain the original accuracy of around 10^{-8} is shown in the subsequent line.

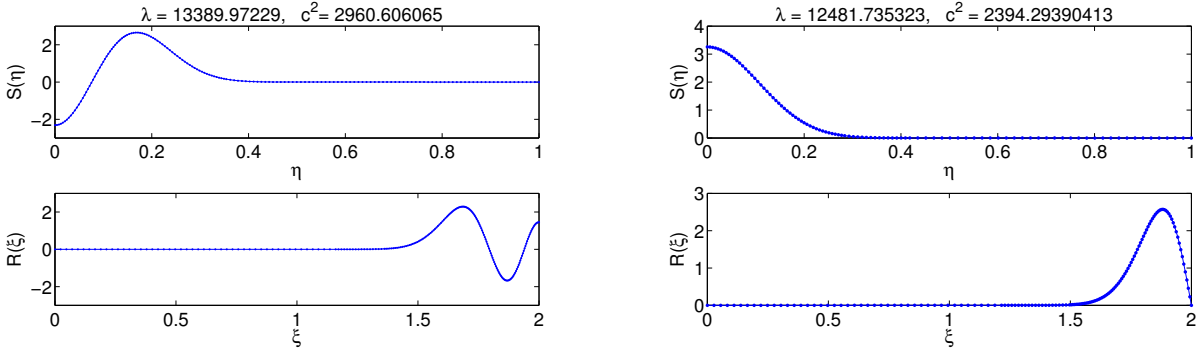


FIGURE 1. $S(\eta)$, $R(\xi)$ obtained on adapted mesh: $m = 100$, $\xi_s = 2$, $l = 2$, $n = 2$, $S'(0) = 0$, $R'(0) = 0$, $R'(\xi_s) = 0$ (left plot), $m = 100$, $\xi_s = 2$, $l = 0$, $n = 0$, $S'(0) = 0$, $R'(0) = 0$, $R(\xi_s) = 0$ (right plot)

TABLE 1. Numerical results on adapted meshes (in bold) and uniform meshes

m	ξ_s	l	n		n_S	n_R	Error $S(\eta)$	Error $R(\xi)$	Error λ	Error c^2
Boundary conditions: $S'(0) = 0$, $R'(0) = 0$, $R'(\xi_s) = 0$										
300	5	2	2	$\lambda = 95631.325979$	196	296	2.30e-10	1.75e-09	1.06e-12	1.91e-11
				$c^2 = 4159.9358440$	196	296	1.28e-06	1.73e-04	8.27e-08	1.86e-06
					800	1000	8.43e-12	1.30e-08	6.00e-12	1.39e-10
500	5	2	2	$\lambda = 263398.416463$	202	517	6.02e-10	1.14e-09	8.38e-13	8.04e-12
				$c^2 = 10947.322763$	202	517	1.20e-05	4.01e-05	2.53e-08	2.76e-07
					800	1200	4.93e-11	5.11e-08	1.38e-11	3.33e-10
100	2	2	2	$\lambda = 13389.97229$	160	208	4.56e-10	1.03e-09	7.69e-12	2.53e-11
				$c^2 = 2960.606065$	160	208	3.93e-08	3.71e-06	1.75e-08	8.11e-08
					600	700	1.35e-12	2.01e-10	9.33e-13	4.36e-12
300	2	2	2	$\lambda = 112982.82771$	204	259	1.56e-10	4.12e-09	6.22e-12	3.19e-11
				$c^2 = 21666.761535$	204	259	8.61e-07	1.71e-04	2.44e-07	1.28e-06
					800	900	2.75e-11	1.01e-08	1.45e-11	7.61e-11
Boundary conditions: $S'(0) = 0$, $R'(0) = 0$, $R(\xi_s) = 0$										
100	2	0	0	$\lambda = 12481.735323$	98	142	5.59e-10	9.20e-11	4.13e-12	2.93e-12
				$c^2 = 2394.29390413$	98	142	1.06e-07	2.18e-07	1.99e-09	5.63e-09
					200	300	1.43e-10	6.78e-11	1.02e-12	1.05e-12

The following conclusion is now in place: The combination of the Prüfer angle technique and high order variable stepsize finite difference schemes allows to efficiently and accurately solve the problem. This result is in agreement with [2, 3, 4]. Using adapted meshes greatly reduces the required number of grid points. This also implies that the discrete problems are of smaller dimension which results in a smaller condition number of matrices involved in the Newton iteration. Consequently, the computed solutions are more accurate.

REFERENCES

1. P. Amodio, G. Settanni, Communications in Nonlinear Science and Numerical Simulation, in press, doi: 10.1016/j.cnsns.2014.05.032
2. P. Amodio, T. Levitina, G. Settanni and E.B. Weinmüller, J. Appl. Math. Comput. **43** (2013), pp. 151–173.
3. P. Amodio, T. Levitina, G. Settanni, E.B. Weinmüller, AIP Conference Proceedings **1558** (2013), Numerical analysis and applied mathematics - ICNAAM 2013. T.E. Simos, G. Psihoyios and Ch. Tsitouras editors, pp. 750-753
4. P. Amodio, T. Levitina, G. Settanni, E.B. Weinmüller, Computer Physics Communications **185** (2014), pp. 1200–1206.
5. M. V. Fedorjuk, Springer Verlag (1993).
6. I. V. Komarov, L. I. Ponomarev, and S. Yu. Slavyanov, Nauka, Moscow (1976).
7. T. V. Levitina, E. J. Brändas, J. Comp. Meth. Sci. & Engrg. **1**, 287–313 (2001).
8. H. Volkmer, Lecture Notes in Mathematics 1356, Springer-Verlag, Berlin, New York (1988).